MD-Vol. 90, CAE and Related Innovations for Polymer Processing, ASME 2000.

ESTIMATION OF ELONGATIONAL VISCOSITY USING ENTRANCE FLOW SIMULATION

Debabrata Sarkar and Mahesh Gupta
Mechanical Engineering-Engineering Mechanics Department
Michigan Technological University
Houghton, MI 49931

ABSTRACT

A new elongational viscosity model along with the Carreau-Yasuda model for shear viscosity is used for a finite element simulation of the flow in a capillary rheometer die. The entrance pressure loss predicted by the finite element flow simulation is matched with the corresponding experimental data to predict the parameters in the new elongational viscosity model. For two different polymers, the predicted elongational viscosity is compared with the corresponding predictions from Cogswell's analysis and K-BKZ model.

INTRODUCTION

Elongational viscosity, which is defined as the ratio of elongational stress to elongational strain rate, characterizes the resistance of a fluid to elongational deformation. For the Newtonian fluids, the ratio of elongational viscosity to shear viscosity (Trouton ratio) is 3 for an axisymmetric elongation and 4 for a planar elongation. Because of their long chain molecules, polymers exhibit a stiff resistance to any elongational deformation. Therefore, the elongational viscosity of a polymer is generally quite high. Since the resistance of a polymer to an elongational deformation changes with molecular alignment during a flow, elongational viscosity of a polymer also depends upon the elongation rate. An accurate knowledge of the elongational viscosity of a polymer is important for simulation of the manufacturing processes such as extrusion, blow molding, fiber spinning, etc. because elongational viscosity can significantly affect the flow of polymer in these processes. However, due to the inherently unsteady nature of an elongational flow, experimental determination of elongational viscosity is difficult. Experimental characterization of the elongational viscosity was pioneered around three decades ago by Meissner [1]. He devised an experimental set-up for generating a controlled uniaxial elongation of a molten polymer. An elongational viscometer based upon Meissner's pioneering work is currently

marketed by Rheometric Scientific, Inc. [2]. Other techniques, such as bubble collapse [3, 4] and stagnation flow [5, 6], have also been used for direct experimental measurement of elongational viscosity. However, since the elongation rate in these experiments cannot be controlled [7], these methods determine only an apparent elongational viscosity. Conceptually, these direct measurement techniques are simple and the elongational viscosity can be easily determined from the experimental data. However, maintaining a steady elongational deformation is difficult at a high elongation rate [8]. Therefore, most experimental data on elongational viscosity in the literature is limited to low elongation rates.

Due to the difficulties associated with direct measurement of elongational viscosity of a polymer, the flow in a channel with abrupt contraction (entrance flow) has often been used for an indirect measurement of elongational viscosity [8]. Since a fluid going through an abrupt contraction experiences a large elongational deformation, entrance flow of a polymer with high elongational viscosity has a steep pressure drop, called entrance pressure loss, near the abrupt contraction. The value to entrance pressure loss, which depends upon the flow rate in the channel, can be used for an indirect measurement of the strain-rate-dependence of the elongational viscosity of a polymer. The advantage of the entrance flow method for measuring elongational viscosity is its applicability at high elongation rate. Furthermore, an existing capillary rheometer, which is commonly used for measuring shear viscosity, can also be used for elongational viscosity estimation. The main difficulty in the use of entrance flow method for measuring elongational viscosity is the complexity of the flow, which, because of the formation of recirculating vortices near an abrupt contraction [8], is particularly difficult to analyze. The effect of various other parameters, such as total strain [9], viscoelastic relaxation [10], and normal stress difference [11], which may also affect the entrance pressure loss, is neglected in this method of elongational viscosity estimation.

By making various simplifying assumptions, several attempts have been made in the literature to analyze the entrance flow. Assuming a shear-free, purely elongational sink flow, Metzner and Metzner [12] obtained the following expressions for the elongational rate ($\dot{\varepsilon}$) and elongational viscosity (η_e):

$$\dot{\varepsilon} = \frac{Q(\sin\phi)^3}{\pi r^3(1-\cos\phi)} \tag{1}$$

$$\eta_e = \Delta p_e / \dot{\varepsilon} \tag{2}$$

where Q denotes the flow rate, r the capillary radius and Δp_e is the entrance pressure loss. The main obstacle in using these equations is the difficulty in finding the half angle of convergence, ϕ, which needs to be determined by flow visualization [13, 14]. Cogswell [15] analyzed the shear as well as elongational flow near an abrupt contraction. By using the force balance to minimize the pressure loss, Cogswell obtained the following equations for estimation of elongational viscosity for an axisymmetric flow:

$$\dot{\varepsilon} = \frac{4\eta_s\dot{\gamma}_a^2}{3(n+1)\Delta p_e} \tag{3}$$

$$\eta_e = \frac{3(n+1)\Delta p_e}{8\dot{\varepsilon}} \tag{4}$$

where $\dot{\gamma}_a = 4Q/(\pi r^3)$ is the apparent shear rate. Cogswell used the power-law model for shear viscosity (η_s):

$$\eta_s = C_s\dot{\gamma}^{n-1} \tag{5}$$

where C_s is the consistency coefficient, $\dot{\gamma}$ is the shear rate and n is the power-law index. In order to minimize the overall energy for an entrance flow, Binding [16], employed the variational principle to obtain the following equation for the entrance pressure loss:

$$\Delta p_e = \frac{2C_s(1+m)^2}{3m^2(1+n)^2}\left[\frac{mC_e(3n+1)n^m I_{nm}}{C_s}\right]^{\frac{1}{m+1}} \dot{\gamma}^{\frac{m(n+1)}{m+1}} \left[1-\alpha^{\frac{3m(n+1)}{m+1}}\right] \tag{6}$$

Where C_e and m define the power-law model for elongational viscosity ($\eta_e = C_e\dot{\varepsilon}^{m-1}$), $\alpha = r/R$ with R and r being the radii of reservoir and capillary respectively, and $I_{nm} = \int_0^1 \left|(3n+1)\rho^{1+1/n}/n - 2\right|^{m+1}\rho d\rho$. If the shear viscosity of a polymer and entrance pressure loss is known, Eqn. (6) can be used to determine the power-law model for elongational viscosity of a polymer.

By using independent power-law models for shear and elongational viscosities, Gupta [17, 18] analyzed the effect of elongational viscosity on vortex formation and entrance pressure loss in an axisymmetric 4:1 entrance flow. In an accompanied paper, Sarkar and Gupta [19] have proposed a new model for the elongational viscosity of a polymer. The model introduced by Sarkar and Gupta [19], which can capture various trends in elongational viscosity, such as an initial increase followed by a descent as the elongational rate is increased, has also been used in this paper. Knowing the shear viscosity and entrance pressure loss for a polymer, the simplex optimization scheme [20] has been used here to determine the four parameters in the elongational viscosity model. The estimated elongational viscosities for two different polymers are reported later in this paper.

SHEAR AND ELONGATIONAL VISCOSITIES

In the present paper, the Carreau-Yasuda equation [21, 22] has been used to model the shear viscosity of a polymer:

$$\eta_s = \eta_o[1+(\lambda e_{II})^a]^{\frac{n-1}{a}} \tag{7}$$

where η_o is the zero-shear-rate viscosity, λ and a define the transition from Newtonian to power–law region, n is the power-law index and $e_{II} = \sqrt{2\tilde{e}:\tilde{e}}$ is the second invariant of the strain-rate tensor $\tilde{e} = (\nabla\hat{v} + \nabla\hat{v}^T)/2$. The elongational viscosity in this paper has been represented by the model proposed by Sarkar and Gupta [19].

$$\eta_e = \eta_o\left[3+\delta\left\{1-\frac{1}{\sqrt{1+(\lambda_1 e_{II})^2}}\right\}\right][1+(\lambda_2 e_{II})^2]^{\frac{m-1}{2}} \tag{8}$$

The elongational viscosity model has four independent parameters, namely, δ, λ_1, m and λ_2. As discussed in the reference [19], the parameter λ_1 in Eqn. (8) specifies $1/e_{II}$ for the transition between Newtonian and elongation-thickening portions of the viscosity strain–rate curve, whereas δ characterizes the total increase in viscosity in the elongation-thickening portion. Parameters λ_2 and m in Eqn. (8) specify $1/e_{II}$ for transition between elongation-thickening and power–law regions, and the power–law index respectively. It should be noted that η_o, the zero-shear-rate viscosity, is the same in Eqns. (7) and (8). Therefore, at low strain-rates, Eqn. (8) enforces the Trouton ratio, $Tr \equiv \eta_e/\eta_s$, to 3, which is based upon the experimental data reported in the literature [8].

ESTIMATION PROCEDURE FOR ELONGATIONAL VISCOSITY PARAMETERS

The procedure for estimation of elongational viscosity starts with an initial guess for the values of four parameters in Eqn. (8). Using the elongational viscosity thus predicted by Eqn. (8) and the Carreau-Yasuda model (Eqn. 7) for shear viscosity, the finite element software reported in reference [17] is employed to predict the entrance pressure loss over the range of flow rate for which the experimental value of Δp_e is available. The simplex optimization scheme [20] is then used to iteratively improve the values of four parameters in Eqn. (8), such that the least-square error between the experimental data for entrance loss and the corresponding estimation from the finite element simulation is minimized (Fig. 1). It should be noted that the error between the experimental data and finite element predictions are minimized for the complete range of flow rate for which the experimental data for Δp_e is available. The simplex optimization scheme is used for a constrained optimization in a semi-infinite search domain with the following limits on the four elongational viscosity parameters.

$$\delta \geq 0 \tag{9}$$

$$n < m \leq 1 \tag{10}$$

$$\lambda_1 > \lambda_2 > 0 \tag{11}$$

A good initial guess for the four parameters in Eqn. (8) is important for success of the optimization scheme. The initial values of the four elongational viscosity parameters should be selected such that the optimized values of the four parameters can be found by "shrinking" the simplex rather than "crawling" in the search domain [20]. In the present work, the initial guess for the four elongational viscosity parameters, given below, is based upon the three parameters (η_o, λ, n) in the Carreau model for shear viscosity (Eqn. 7):

Parameter	Simplex Node 1	Simplex Node 2
δ	10	100
λ_1	100λ	1000λ
λ_2	$\lambda/1000$	$\lambda/100$
m	$(2n+1)/3$	$(n+2)/3$

The optimization procedure discussed above has been used in the present work to develop a software for estimation of the elongational viscosity of a polymer. For two polymer melts, the estimated elongational viscosity using this software is reported in the next section.

ESTIMATED ELONGATIONAL VISCOSITY

In this section, the elongational viscosities for two different polymers, namely, Dowlex 2049 and M-LLDPE, are estimated. To determine the elongational viscosity of a polymer, the parameter estimation procedure discussed in the last section requires the experimental data for entrance pressure loss and shear viscosity of the polymer. In this section, the required data for Dowlex 2049 and M-LLDPE has been obtained from reference [24] by Mitsoulis et al. Mitsoulis et al. [24] used a die with 90 degrees entrance angle, and the reservoir and capillary diameters of 9.5 mm and 1.27 mm, respectively. To simulate the flow in the capillary rheometer, a finite element mesh for the same channel geometry was generated in the present work. For Dowlex 2049, the Carreau model parameters given by Mitsoulis et al. (η_o = 7897.7 Pa.s, λ = 1.689 s, n = 0.722) were used for the flow simulation (Fig. 3). Using these parameters for shear viscosity and the experimentally determined entrance pressure loss, the elongational viscosity based upon the optimized values of four parameters (δ = 5.594, λ_1 = 2.848 s, λ_2 = 0.437 s, m = 0.759) is shown in Fig. 3. The corresponding prediction of entrance pressure loss from the finite element simulation is shown in Fig. 2. Since the objective of the simplex optimization scheme is to minimize the error between the experimentally determined and predicted entrance pressure loss, as

expected, the entrance pressure loss predicted by the finite element flow simulation is in good agreement with the experimental data of Mitsoulis et al. [24]. Mitsoulis et al. used the K-BKZ constitutive equation to simulate the entrance flow. Their predictions of entrance pressure loss and elongational viscosity, using the K-BKZ model, are also shown in Fig. 2 and Fig. 3, respectively. The entrance pressure loss predicted by the K-BKZ model is significantly lower than the corresponding experimental data. At low strain rate, the experimentally determined elongational viscosity was also reported by Mitsoulis et al. [24]. The experimental data further confirms the Trouton ratio of 3 at low strain rates, which is also predicted by K-BKZ model as well as the elongational viscosity estimated in the present work. The elongational viscosity predicted by Cogswell's analysis (Eqns. 3 and 4), which is also shown in Fig. 3 is in reasonable agreement with the elongational viscosity predicted in the present work.

Even though, for Dowlex 2049, the predicted entrance pressure loss in Fig. 2 is in good agreement with the corresponding experimental data, if the elongational viscosity predicted by the optimized parameters is used to simulate another entrance flow with a different contraction ratio or different convergence angle, the predicted entrance loss may not agree with the corresponding experimental data. In other words, if the elongational viscosity estimated by the entrance flow simulation is a good estimate of the intrinsic elongational viscosity of the polymer, then the elongational viscosities estimated by different entrance flow simulations with different contraction ratio or entrance angle, should be in good agreement. For M-LLDPE, Mitsoulis et al. [24] reported the experimental data for entrance pressure loss for three different contraction ratios (Fig. 5). Keeping the reservoir diameter (9.5 mm) the same, three different orifice diameters (d = 0.508, 0.762 and 1.27 mm) were used. For all three contraction ratios, the entrance angle is 90^o. The entrance pressure loss data for the three different contraction ratios was used in the present work to obtain three different estimates of the elongational viscosity. The shear viscosity data from Mitsoulis et al. [24] was used to determine the Carreau-Yasuda model parameters (η_o = 29880 Pa.s, λ = 0.1077 s, n = 0.226, a = 0.493) for M-LLDPE (Fig. 5). The predicted elongational viscosity for the three contraction ratios and the corresponding predictions of entrance pressure loss are shown in Fig. 5 and Fig. 4, respectively. The optimized elongational viscosity parameters for the three elongational viscosity curves shown in Fig. 5 are as follows.

d (mm)	δ	λ_1 (s)	λ_2 (s)	m
0.508	1.844	0.0663	0.0596	0.229
0.762	1.962	5.7768	0.0593	0.227
1.270	2.639	0.4704	0.0487	0.226

In the power-law region of the elongational viscosity ($e_{II} > 1/\lambda_2$), the elongational viscosities predicted by using the entrance pressure loss data for the three different contraction ratios are in good agreement. However, the predicted elongation-thickening regions for the three cases are quite different. Since the entrance pressure data in Fig. 5 is mostly in the power-law region, the predicted elongational viscosity in the elongation-thickening region is expected to have some error. The entrance pressure loss data at lower strain-rates is required to improve the accuracy of the elongational viscosity in the elongation-thickening region. However, at low strain rates, the entrance pressure loss may be too small to measure accurately. The entrance pressure loss and elongational viscosity predicted by Mitsoulis et al. [24] using K-BKZ model, are also shown in Figs. 4 and 5, respectively. Even though the entrance pressure loss predicted by the K-BKZ model is in reasonable agreement with the experimental data, the elongational viscosity predicted by the K-BKZ model is much higher than the viscosity estimated in the present work. The elongational viscosity predicted by using the Cogswell's analysis (Eqns. 3 and 4), which envelops our predictions in the elongational thickening region, is slightly higher than the elongational viscosity in the power-law region predicted in the present work.

CONCLUSIONS

The simplex algorithm has been used to optimize the values of four rheological parameters in a new elongational viscosity model. The optimization scheme iteratively improves the value of the elongational viscosity parameters by minimizing the difference between the entrance pressure loss predicted by a finite element simulation of the flow in a capillary rheometer and the corresponding experimental data. Elongational viscosity for Dowlex 2049 and M-LLDPE was predicted. The elongational viscosity of M-LLDPE predicted by using the entrance pressure loss data for the three different contraction ratio in a capillary rheometer are in good agreement in the power-law region of the elongational viscosity. Since the experimental data for entrance pressure loss data is mostly limited to the power-law region, the elongation-thickening region of the viscosity curves obtained by using the experimental data for different contraction ratio is quite different. In view of the difficulties associated with the direct experimental measurement of elongational viscosity, the method proposed here provides an attractive alternative for estimation of the elongational viscosity of a polymer.

REFERENCES

1. Meissner, J., *Rheol. Acta*., **8**, 78 (1969).
2. Rheometrics Scientific, Inc. One Possumtown Road, Piscataway, NJ 08854, USA (http://www.rheosci.com).
3. Pearson, G. H. and Middleman, S., *AIChE J.*, **23**, 714 (1977).
4. Johnson, E. D. and Middleman, S., *Polym. Eng. Sci.*, **18**, 963 (1978).
5. Taylor, G. I., *Proc. R. Soc.*, **A146**, 501 (1934).
6. Cai, J., Souza Mendes, P. R., Macosko, C. W., Scriven, L. E., Secor, R. B., in *Theoretical and Applied Rheology*, Moldenaers, P., Keunings, R. (Eds.), Elsevier, 1012 (1992).
7. Tirtaatmadja, V. and Sridhar, T., *J. Rheol.*, **37**, 1081 (1993).
8. Macosko, C. W., *Rheology Principles, Measurements and Applications*, VCH, New York (1994).
9. Petrie, C. J. S., *J. Non–Newtonian Fluid Mech.*, **70**, 205 (1997).
10. Spiegelberg, S. H. and McKinley, G. H., *J. Non–Newtonian Fluid Mech.*, **67**, 49 (1996).
11. Debbaut, B. and Crochet, M. J., *J. Non-Newtonian Fluid Mech.*, **30**, 169 (1988).
12. Metzner, A. B. and Metzner, A. P., *Rheol. Acta*, **9**, 174 (1970).
13. Denn, M. M., in *The Mechanics of Viscoelastic Fluids*, Rivlin, R. S. (ed.), ASME, New York (1977).
14. Cogswell, F. N., *J. Non–Newtonian Fluid Mech.*, **4**, 23 (1978).
15. Cogswell, F. N., *Polym. Eng. Sci.*, **12**, 64 (1972).
16. Binding, D. M., *J. Non-Newtonian Fluid Mech.*, **27**, 193 (1988).
17. Gupta, M., *SPE ANTEC Tech. Papers*, **45**, 1254 (1999).
18. Gupta, M., *Polym. Eng. Sci.*, **40**, 23 (2000).
19. Sarkar, D. and Gupta, M., "An Investigation of the Effect of Elongational Viscosity on Entrance Flow," Submitted for presentation at ASME-IMECE 2000.
20. Nelder, J. A. and Mead R., *Computer J.*, **7**, 308 (1965).
21. Carreau, P. J., Ph.D. Thesis, University of Wisconsin, Madison (1968).
22. Yasuda, K., Ph.D. Thesis, MIT, Cambridge (1979).
23. Munstedt, H. *J. Rheol.*, **24**, 847 (1980).
24. Mitsoulis, E., Hatzikiriakos, S. G., Christodoulou, K. and Vlassopoulos, D., *Rheol. Acta*, **37**, 438 (1998).

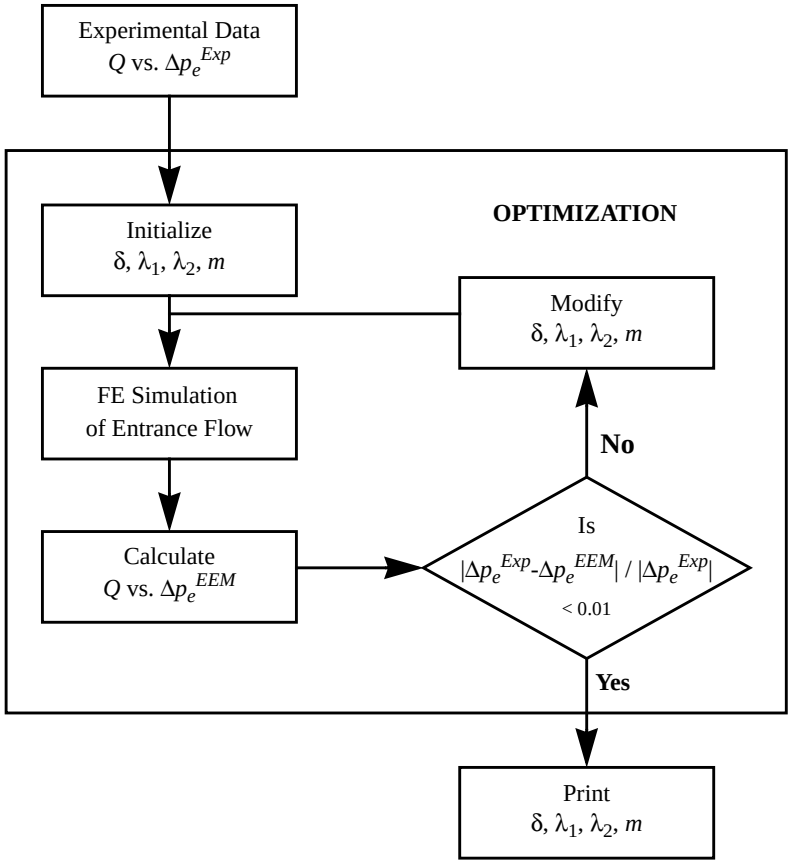

Fig. 1. Flow chart for optimization of elongational viscosity parameters.

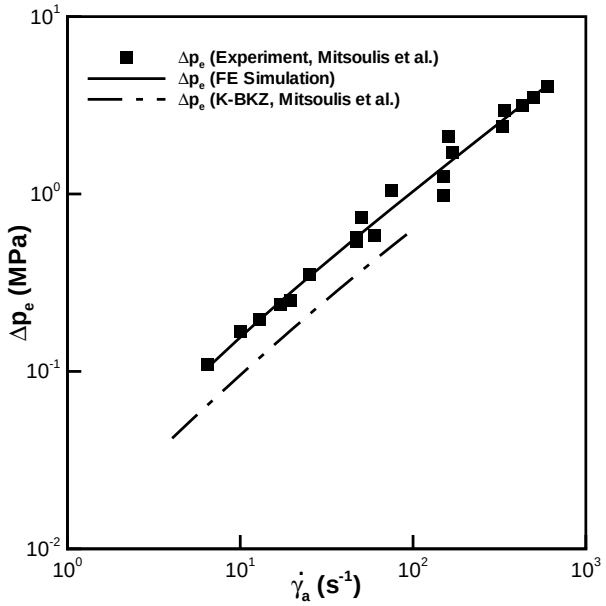

Fig. 2. Entrance loss vs. apparent shear rate for Dowlex 2049 at 200^{o}C.

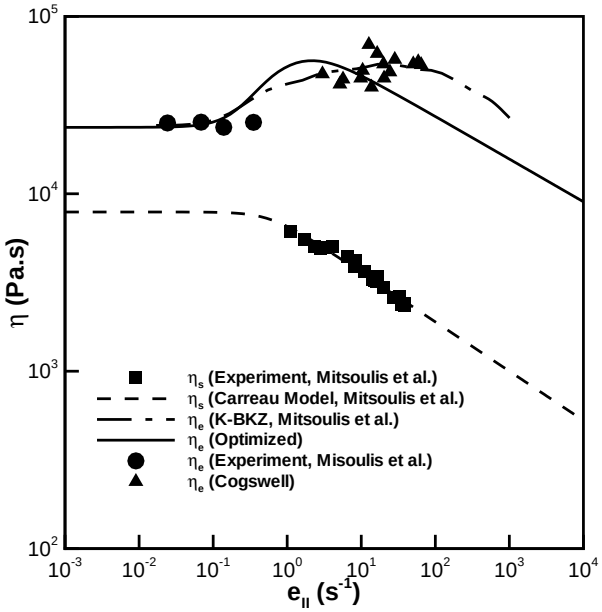

Fig. 3. Variation of shear (η_s) and elongational (η_e) viscosities of Dowlex 2049 at 200^{o}C with the second invariant of strain-rate tensor (e_{II}).

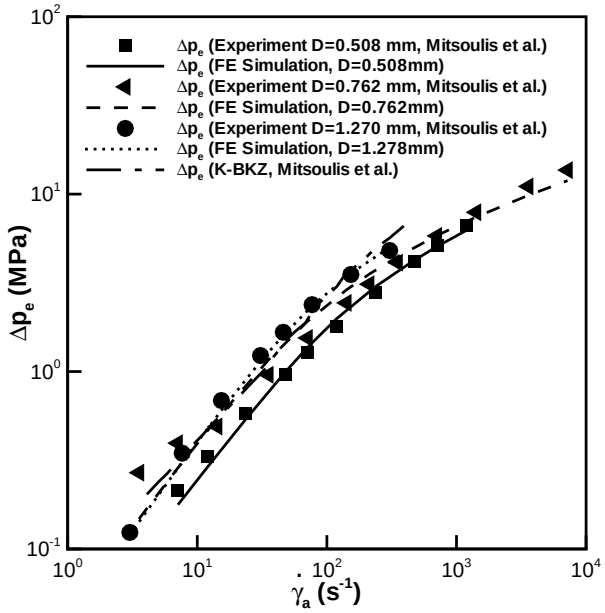

Fig. 4. Entrance loss vs. apparent shear rate for M-LLDPE at 150^{o}C.

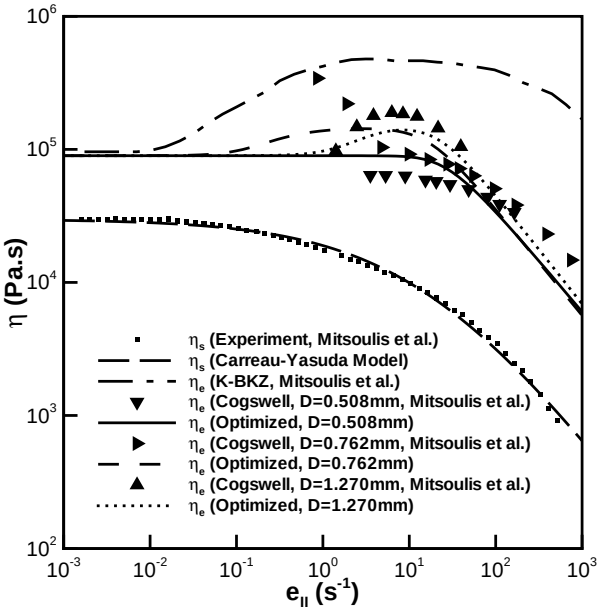

Fig. 5. Variation of shear (η_s) and elongational (η_e) viscosities of M-LLDPE at 150^{o}C with the second invariant of strain-rate tensor (e_{II}).